Archives of Materials Science and Engineering

Volume 28
Issue 4
April 2007
Pages 203-210

International Scientific Journal
published monthly as the organ of
the Committee of Materials Science
of the Polish Academy of Sciences

Structure and precipitation strengthening in a high-temperature Fe–Ni alloy

K.J. Ducki *
Materials Science Department, Silesian University of Technology,
ul. Krasińskiego 8, 40-019 Katowice, Poland
* Corresponding author: E-mail address: kazimierz.ducki@polsl.pl

Received 21.10.2006; accepted in revised form 20.02.2007

ABSTRACT

Purpose: The relationships between the kinetics of precipitation and growth of the intermetallic phase γ' [Ni_3(Al,Ti)] and the strengthening magnitude obtained in a high-temperature Fe–Ni alloy of the A-286 type has been studied. In order to accomplish the goal of the study, the author used the LSW coagulation theory and Brown and Ham's conventional analysis of strengthening by ordered particles.

Design/methodology/approach: The samples were subjected to a solution heat treatment at 980°C/2h/water and then aged at 715, 750, and 780°C, with holding times 0.5-500h. The heat-treated samples were subjected to structural analyses (TEM, X-ray diffraction) and analyses of mechanical properties (hardness test, static tensile test, and impact test).

Findings: Direct measurements on the electron micrographs allowed to calculate the structural parameters of the γ' phase, i.e. mean diameter, volume fraction and mean distance between particles. In accordance with the LSW theory, linear dependencies of changes in mean diameter as a function of aging time (t1/3) were elaborated. The author carried out analyses of strengthening and flow stress ($\Delta\tau$) increases as a function of the particle size of the γ' phase and determined the value of the antiphase boundary energy (γ_{APB}) for the analyzed Fe–Ni alloy.

Practical implications: The obtained relationships of the growth of the γ' phase particles as a function of temperature and aging time can be used to determine the magnitude of strengthening and flow stress in high-temperature Fe–Ni alloys during extended aging or usage.

Originality/value: This study exploits LSW coagulation theory and Brown and Ham's conventional analysis to describe precipitation strengthening by ordered particles of the intermetallic phase γ' in a high temperature Fe–Ni alloy.

Keywords: Metallic alloys; Heat treatment; Structure; Precipitation strengthening

MATERIALS

1. Introduction

High-temperature Fe–Ni alloys that have been precipitation strengthened by intermetallic phases display numerous characteristic properties, i.e. [1-3]: excellent mechanical properties, considerable creep resistance and heat resistance at slightly elevated and high temperatures, excellent corrosion resistance, high ductility at low temperatures, and are non-magnetic. The temperatures at which these alloys are applicable range from the temperature of liquid helium (-269°C) to 540-815°C. This group of modern metallic materials have found an increasingly wide range of applications in conventional and nuclear power industry, in aviation technology, in chemical and petrochemical industries, and in cryogenic engineering; additionally, they are used for tools in non-ferrous metal processing.

The principal strengthening phase, which is precipitated in creep resisting Fe–Ni alloys, is the intermetallic phase γ'[Ni_3(Al,Ti)]. In the initial stages of aging, this phase precipitates in the form of zones and dispersive particles, which are coherent with the matrix. Diffusive processes of growth and coagulation of the phase γ' particles as well as overageing, which is primarily related to the γ'→ η[Ni_3Ti] transformation, occur during the subsequent stages of aging or usage. The process of growth of the

phase γ' particles for coagulation controlled with volume diffusion can be described using LSW (Lifshitz–Slyozov–Wagner) theory [4, 5]. The LSW coagulation theory proposes that the average diameter of precipitates increases with the cube root of ageing or usage time.

In Fe–Ni alloys that have been precipitation strengthened with the intermetallic phase γ', the intensity of strengthening depends on the following factors [6, 7]: antiphase boundary (APB) and error energy of the phase γ' arrangement, strength of the matrix (γ) and the γ' phase, cohesion stress γ/γ', volume fraction of the γ' phase, particle size of the γ' phase, indexes of diffusion in γ and γ' phases, and degree of the γ/γ' lattice misfit. Among the above-mentioned factors, cohesion stress occurring between the γ' phase particles and the matrix were for a long time considered the most significant for precipitation strengthening. However, according to numerous authors [6-10], the γ' phase is coherent with austenite but cohesion stresses are insignificant and should not be considered the primary factor of the strength increase in this group of alloys.

Application of Brown and Ham's [9] conventional analysis in describing precipitation strengthening enables the determination of the impact of the γ' phase precipitates on the value of critical shear stress or yield point of the aged Fe–Ni alloys. Strengthening by ordered particles of the γ' type is associated with the occurrence of antiphase boundary (APB) on the slip plane of a particle cut by dislocation. The energy of APB per unit area (γ_{APB}) describes a force suppressing the dislocation motion per unit of its length when moving through a particle. According to numerous researchers [8-10], the activity of antiphase boundaries within incompletely ordered particles of the γ' phase is the most important mechanism of precipitation strengthening in Fe–Ni alloys.

In work applied LSW coagulation theory and Brown and Ham's conventional analysis to describe the precipitation strengthening by ordered particles of the γ' phase in a high-temperature Fe–Ni alloy of the A-286 type during heat treatment. The growth index of the γ' phase particles as a function of ageing parameters was identified, the increase in strength and flow stress of the alloy as a function of particle size of the γ' phase was analyzed, and value of APB energy was determined.

2. Material and procedure

Rolled bars, 16 mm in diameter, of an austenitic Fe–Ni alloy designated X5NiCrTi26-15 were studied. The chemical composition of the material is given in Table 1.

The samples for testing cut off these rods were subjected to solution heat treatment at 980°C for 2 h and water quenched, and then to aging at temperatures 715, 750 and 780°C at holding time from 0.5 to 500 h.

The structural examinations were carried out using thin foil technique on a Jeol JEM-2000 FX transmission electron microscope (TEM). The X-ray phase analysis of isolates was carried out with a Philips PW-1140 X-ray diffractometer.

The quantitative analysis of secondary γ' phase particles, which phase precipitated in the alloy during ageing, was performed on TEM images in bright field mode. Based on direct counting, basic stereological parameters of the γ' phase were determined from binary images, i.e.: the mean diameter ($\overline{D}$), the volume fraction particles (V_V) and the mean distance between particles (l_d).

The mean diameter ($\overline{D}$) of the particles was evaluated with help of the relation given by Czyrska-Filemonowicz *et al*. [11] and Wasilkowska *et al*. [12]:

$$\overline{D} = \frac{\overline{d}t}{t - \overline{d} + \left(\pi A_A / L_A\right)} \tag{1}$$

where: $\overline{d}$ – the mean diameter of the circles in the projected plane (nm), t – the foil thickness (nm), A_A – the projection area, L_A – the perimeter density (1/nm).

The volume fraction (V_V) of γ' particles was calculated using the formula provided by Dubiel *et al*. [13]:

$$V_V = \frac{\pi}{6}\frac{\sum N_i d_i^3}{A\left(t + \overline{d}\right)} \tag{2}$$

where: N_i – the number of particles with diameter d_i, A – the total projection area (nm^2).

The mean distance between particles (l_d) was estimated using the equation given by Schröder and Arzt [14]:

$$l_d = \overline{d}\sqrt{\frac{\pi}{6V_V}\left(1 + \frac{s^2}{\overline{d}^2}\right)} - \frac{\pi}{4}\overline{d} \tag{3}$$

where: s – the standard deviation of the particle diameter distribution.

The analysis of the γ' phase growth step was made on the basis of the LSW theory for coagulation on volume diffusion controll according to the relationship provided by Kusabiraki *et al*. [15]:

$$\overline{d}^3 - \overline{d}_0^3 = \frac{64\sigma D C_e V_m^2}{9RT} = K't \tag{4}$$

where: $\overline{d}$ and $\overline{d}_0$ – average diameter of precipitates at time t and t = 0 respectively, σ – interfacial energy between precipitates and matrix, D – diffusion coefficient of the solute atom in the matrix, C_e – concentration of solute atoms in the matrix in equilibrium with a particle of an infinite size, V_m – molar volume of precipitation phase, R – gas constant, T – absolute temperature, K' – growth rate constant.

The hardness measurements of samples made by Vickers method at 98 N load were performed using a Zwick hardness tester coupled with a PC class computer. The static tensile test of samples were performed on MTS testing machine with extensometric measurement of elongation. Impact measurements of Charpy V samples were made using an impact hammer of PSW-30 type with initial energy 294 J.

Flow stress increments (Δτ) for aged Fe–Ni alloy were plotted as a function of square root of γ' particle size in accord with the Brown and Ham [9, 10] conventional analysis for ordered-particle strengthening:

Table 1.
Chemical composition of the investigated alloy

Content of an element [wt.%]														
C	Si	Mn	S	P	Cr	Ni	Mo	W	V	Ti	Al	Co	B	N
0.050	0.55	1.25	0.016	0.026	14.3	24.5	1.34	0.10	0.41	1.88	0.16	0.08	0.007	0.0062

$$\Delta\tau = \frac{1}{2b}\cdot\left(\frac{df}{T}\right)^{1/2}\cdot(\gamma_{APB})^{3/2} - \frac{f}{2b}(\gamma_{APB}) \quad (5)$$

where: d – particle diameter, f – particle volume fraction, b – matrix Burgers vector, T – dislocation line tension, γ_{APB} – anti-phase boundary (APB) energy.

3. Experimental result

The examined Fe–Ni alloy, after heat solution treatment (980°C/2h/water), has the structure of twinned austenite with increased dislocation density and a small amount (ca. 0.3%) of undissolved precipitates (Fig.1). The following titanium compounds occurred in the phase composition of undissolved precipitates: carbide TiC, nitride TiN, carbonitride Ti(C,N), carbosulfide $Ti_4C_2S_2$, Laves phase Ni_2Si, and boride MoB [16].

In the supersaturated state, the alloy was characterized with decreased hardness (HV=180-184) and moderate strength properties (P.S.=295-301 MPa, T.S.=631-651 MPa). This was accompanied by increased plastic properties (EL.=37-42%, R.A.=65-68%) and high impact strength (KCV=180-190 J/cm^2). Application of 1 × step ageing at 715, 750, and 780°C after heat solution treatment and holding times ranging from 0.5 to 500 h results in the processes of precipitation of intermetallic phases of the γ'[Ni_3(Al,Ti)], η[Ni_3Ti], G[$Ni_{16}Ti_6Si_7$], β[NiTi], and σ[$Cr_{0,46}Mo_{0,40}Si_{0,14}$] types and of $M_{23}C_6$ carbide in the Fe-Ni alloy [16]. The intermetallic γ' phase was the primary phase precipitated during alloy ageing. This phase, in the initial stages of ageing at 715°C, precipitated homogeneously in the form of zones and dispersive particles coherent with the matrix, which, according to Pickering [8], is related to spinoidal decomposition of supersaturated austenite (Fig. 2).

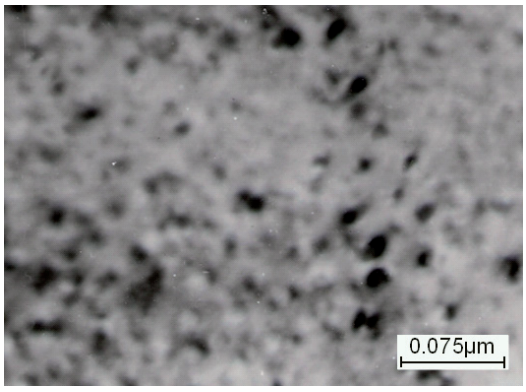

Fig. 2. Structure of the alloy after solution heat treatment and aging at 715°C/4h. Coherent zones and metastable precipipitates of γ' phase in the matrix

Intensive precipitation of dispersive and spheroidal γ' phase particles characterized by strong cohesion with austenite was observed in the alloy matrix at longer ageing times (Fig. 3).

Increase in the aging temperature to 750°C intensified the diffusive processes of growth and coagulation of the γ' phase particles, which still retain a spheroidal shape and cohesion with austenite (Fig. 4). At the highest ageing temperature of 780°C, a clear effect of overageing, associated with coagulation of the γ' phase particles, loss of cohesion with austenite and occurrences of arrangement errors inside the precipitates were observed in the alloy structure (Fig. 5). The following compounds were revealed in the phase composition of extracted precipitates: carbide TiC, carbonitride Ti(C,N), nitride TiN, carbosulfide $Ti_4C_2S_2$, boride MoB, and Laves phase Ni_2Si [16].

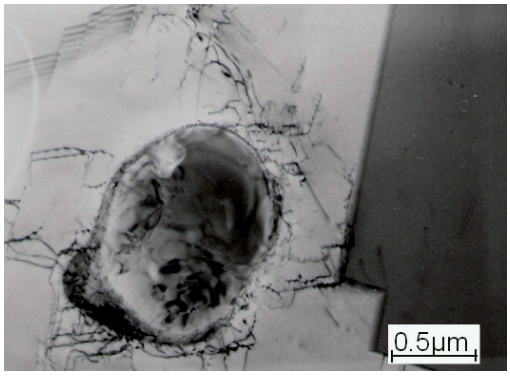

Fig. 1. Structure of the alloy after solution heat treatment at 980°C/2h/w. Twinned austenite with increased dislocation density and undissolved particle

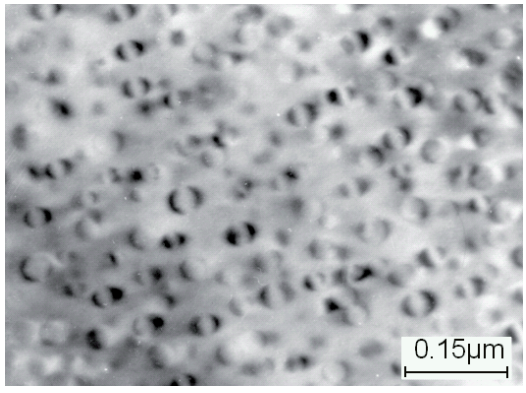

Fig. 3. Structure of the alloy after solution heat treatment and aging at 715°C/150h. Coherent spheroidal γ' phase precipitates in the matrix

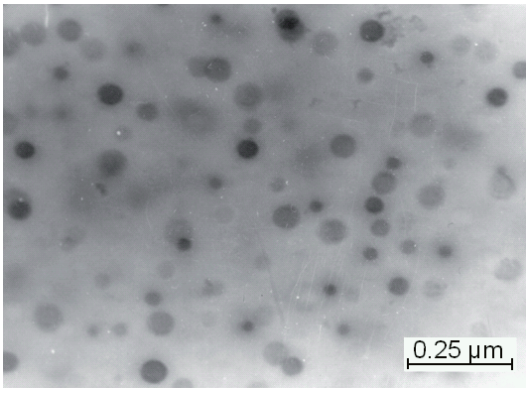

Fig.4. Structure of the alloy after solution heat treatment and aging at 750°C/300h. Diversified size of spheroidal γ' phase particles in the matrix

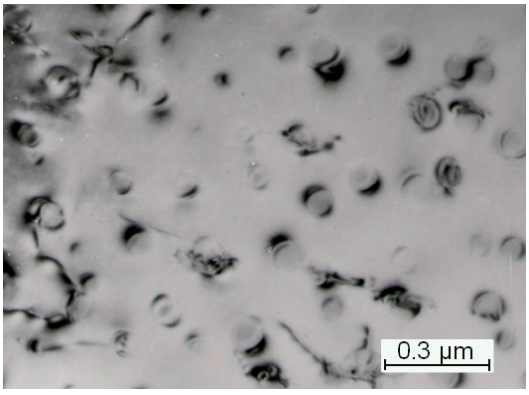

Fig. 5. Structure of the alloy after solution heat treatment and aging at 780°C/500h. Coagulated spheroidal γ' phase particles in the matrix

Quantitative analysis of particles of the γ' phase precipitated in the alloy during ageing was conducted at the ageing temperatures of 715, 750, and 780°C and holding times ranging from 4 to 500 h. For ageing times below 4h, only coherent zones occurred in the alloy matrix and quantitative analysis of the γ' phase was not conducted. Table 2 presents results of the quantitative analysis of the γ' phase obtained for selected ageing times, i.e. 4, 150, 300, and 500 h. It is evident from the presented data that at an ageing temperature of 715 °C and holding times of 4-500h the mean diameter of particles ($\overline{D}$) increased from 7.5 to 23 nm, while the volume fraction changed increased from 10.6 to 45.1 nm and the volume fraction from 0.1 to slightly from 0.07 to 1.4%. For the higher ageing temperature of 750°C and the same holding times, the mean particle diameter2.1%. The mean particle diameter reached the greatest values, ranging from 13.1 to 80.5 nm, with the greatest range of volume fraction, from 0.4 to 8.4%.

The course of growth and coagulation processes of the γ' phase was analyzed based on LSW theory according to equation (4). The relationship between the mean diameter ($\overline{D}$) of the γ' phase particles and ageing time raised to the one third power ($t^{1/3}$) at the aging temperatures of 715, 750, and 780°C is presented in Fig.6. Linear regressions were obtained for all analyzed temperatures, which demonstrates that coagulation of the γ' phase particles occurs according to LSW theory and is controlled by volume diffusion. The regression slopes increase with rising temperature of ageing, which can be explained by an increase in rates of particle coagulation and growth. In the case of the shortest analyzed ageing times, i.e. 0.5 and 2h, the mean values of diameters ($\overline{D}$) of the γ' phase precipitates were obtained through extrapolation.

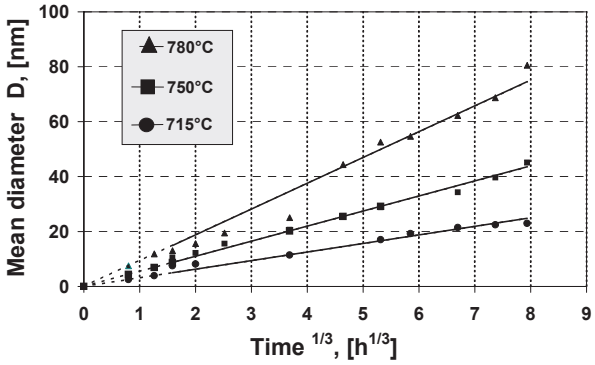

Fig. 6. Relationship between the mean diameter of γ' phase particles and the cube root of aging time at temperatures of 715, 750 and 780°C

The processes of precipitation, growth, and coagulation of intermetallic phases and carbides that occurred during ageing had an essential impact on the alloy's mechanical properties. Ageing of the alloy at 715°C resulted in a clear increase in hardness, improvement of mechanical properties, and a moderate deterioration of plastic properties (Figs.7-10). A particularly intensive increase in hardness and strength of the alloy occurred during the initial stages of aging with short holding times, i.e. 0.5-2h, which was accompanied by a clear deterioration of its plastic properties and impact strength. The highest values of hardness (HV=324) and mechanical properties (P.S.=710 MPa, T.S.=1035 MPa) with moderate values of plastic properties (EL.=26%, R.A.=48%) and impact strength (KCV=97 J/cm^2) were obtained in the alloy aged at 715°C for 16h. These conditions produce ca. 78% increase in hardness, 64% increase in tensile strength, and 140% increase in yield.

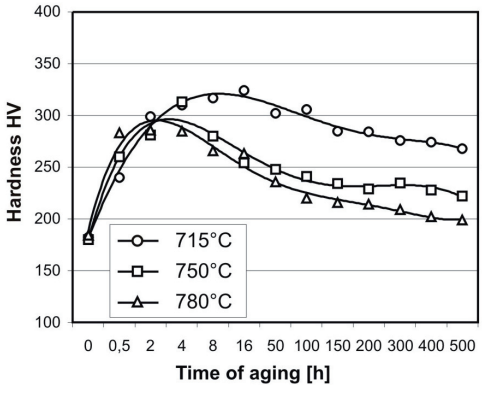

Fig. 7. Course of alloy hardness with aging time at 715, 750 and 750°C temperatures

Table 2.
Stereological parameters of the γ' particles in the tested alloy

Stereological parameters	Time of aging [h] at 715°C					Time of aging [h] at 750°C					Time of aging [h] at 780°C				
	4	50	150	300	500	4	50	150	300	500	4	50	150	300	500
A_A [%]	2.1	6.0	16.5	9.8	10.9	3.2	17.7	11.5	13.3	15.6	5.6	5.3	11.5	10.0	9.5
$\bar{d}$ [nm]	7.4	10.5	25.7	18.7	19.9	9.2	18.9	24.3	28.6	36.6	12.7	24.3	47.2	53.6	70.7
$\bar{D}$ [nm]	7.5	11.4	17.1	21.5	23.0	10.6	20.6	28.8	34.3	45.1	13.1	25.1	52.5	62.3	80.5
V_V [%]	0.07	0.3	1.0	1.1	1.4	0.1	1.2	1.1	1.5	2.1	0.4	2.3	7.7	7.8	8.4
l_d [nm]	195	144	106	127	121	217	115	128	155	164	153	103	89	103	124

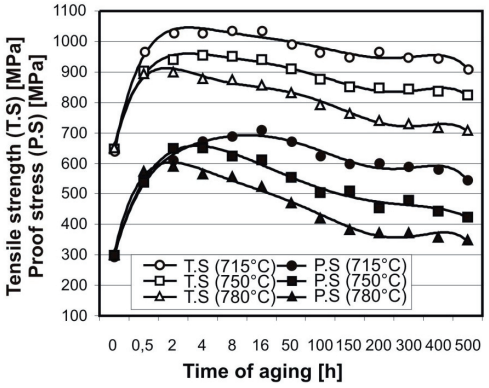

Fig. 8. Course of mechanical properties of alloy with aging time at 715, 750 and 780°C temperatures

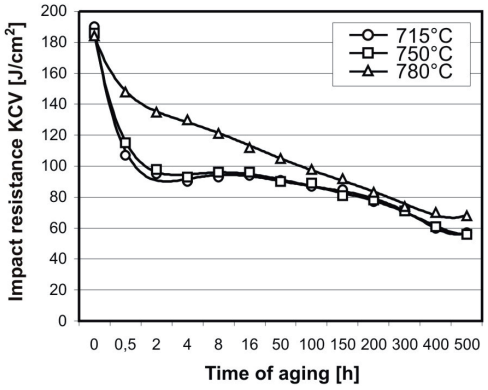

Fig. 10. Course of impact resistance of alloy with aging time at 715, 750 and 780°C

strength in comparison to the supersaturated state. A moderate decline in hardness and mechanical and plastic properties was observed at longer holding periods ranging from 50 to 500h. The lowest values of hardnes (HV=268) as well as mechanical (P.S.=548 MPa, T.S.=913 MPa) and plastic properties (EL.=26%, R.A.=48%, KCV=57 J/cm^2) were obtained in the alloy after the longest aging time, 500h.

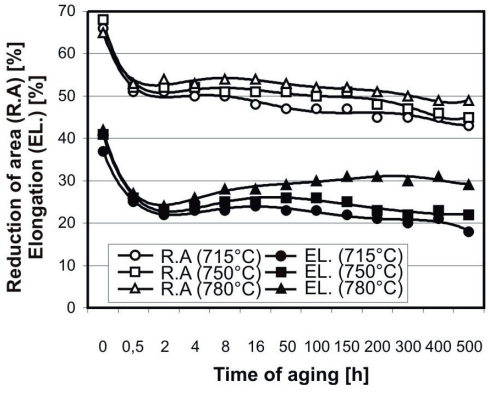

Fig. 9. Course of plastic properties of alloy with aging time at 715, 750 and 780°C temperatures

An increase in the ageing temperature to 750°C resulted in a less significant increase in hardness and strength and a comparable decline in plastic properties (Figs. 7-10). Also, in this case, the most intensive increase in alloy hardness and strength as well as the decline of plastic properties were observed in the initial stage of ageing, that is, at short holding times ranging from 0.5 to 2h. The maximal values of hardness (HV=313) and mechanical properties (P.S.=651 MPa, T.S.=955 MPa) with moderate values of plastic properties (EL.=23%, R.A.=52%) and impact strength (KCV=93 J/cm^2) were obtained in the alloy aged at 750°C for 4h. These conditions produce a ca. 74% increase in hardness, a 47% increase in tensile strength, and a 118% increase in yield strength in comparison to the supersaturated state. A moderate decline in alloy hardness as well as mechanical and plastic properties was observed at longer holding periods, ranging from 8 to 500h. Minimum values of hardness (HV=222) as well as mechanical (P.S.=424 MPa, T.S.=817 MPa) and plastic properties (EL.=22%, R.A.=45%, KCV=56 J/cm^2) were obtained in the alloy with the longest ageing time, i.e. 500h.

For the highest ageing temperature, 780°C, the investigated alloy was characterized by the smallest increase in hardness and strength and a slight improvement of its plastic properties (Figs. 7-10). Also in this case, the most intensive increase in alloy hardness and strength occurred in the initial stage of ageing at short holding times ranging from 0.5 to 2h. The highest values of hardness (HV=286) and mechanical properties (P.S.=591 MPa, T.S.=899 MPa) with moderate values of plastic properties (EL.=24%, R.A.=54%) and impact strength (KCV=135 J/cm^2) were obtained in the alloy aged at 780°C for 2h. These conditions produced a ca. 55% increase in hardness, a 38% increase in tensile strength, and a 96% increase in yield strength in comparison to the supersaturated state. A moderate decline in mechanical properties and a slight improvement in plastic properties were observed at longer holding

periods, ranging from 4 to 500h. The lowest values of hardness (HV=199) as well as mechanical (P.S.=349 MPa, T.S.=708 MPa) and plastic properties (EL.=29%, R.A.=49%, KCV=68 J/cm^2) were obtained in the alloy with the longest ageing time, 500h.

Precipitation strengthening of the Fe–Ni alloy during ageing was described based on results from the structural analysis and investigation of mechanical properties. The initial analysis included plotting graphs of increases in hardness (ΔHV), yield strength (ΔP.S.), and tensile strength (ΔT.S.) as a function of change in the γ' phase particle size, i.e. the mean diameter ($\overline{D}$). These graphs were based on the heated equivalent diameter of the γ' phase particles included in table 2 as well as the mean values of hardness (HV) and mechanical properties (P.S and T.S.) presented in Figs. 7-10. The values of $\overline{D}$ that are missing for the shortest and some longer ageing times were obtained through extrapolation, which was conducted based on LSW theory (Fig. 6). The obtained increases in hardness (ΔHV), yield strength (ΔP.S.), and strength (ΔT.S.) as a function of the mean diameter ($\overline{D}$) of the γ' phase particles are presented in Figs.11-13. It is evident from the plotted curves that the level of strengthening obtained during ageing was highly correlated with the average diameter of the γ' precipitates and the ageing temperature. The greatest increases in hardness (ΔHV=130-142) and strength (ΔP.S.=375-415 MPa, ΔT.S.=399-404 MPa) were obtained for the ageing temperature of 715°C and particle size of 7.5-9.5 nm. Slightly less significant increases in hardness (ΔHV=100-133) and strength (ΔP.S.=325-350 MPa, ΔT.S.=304- 308 MPa) were noted for the ageing temperature of 750°C and somewhat larger diameters of the γ' phase precipitates, 9-12 nm. The least significant increases in hardness (ΔHV=100-102) and strength (ΔP.S.=265-290 MPa, ΔT.S.=227-248 MPa) occurred for the highest ageing temperature, 780°C, and slightly larger diameters of the γ' phase precipitates ranging from 10 to13 nm.

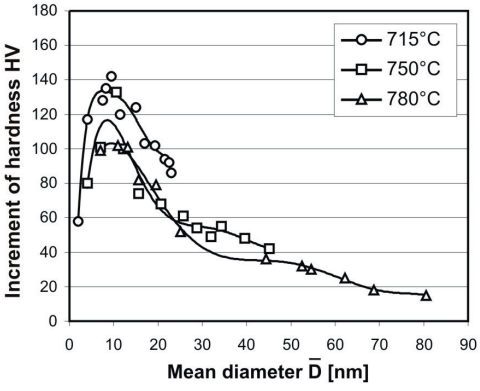

Fig.11. Relations between increased hardness and mean diameter of γ' precipitates

The second stage of the alloy strengthening analysis included application of the conventional theory of precipitation strengthening by ordered particles, which was proposed by Brown and Ham [9]. The increase in flow stress (Δτ) for the tested alloy was analyzed according to equation (5) of this article. In order to determine the values of flow stress for the tested alloy, it was necessary to solve for Δτ from the equation [9,10]:

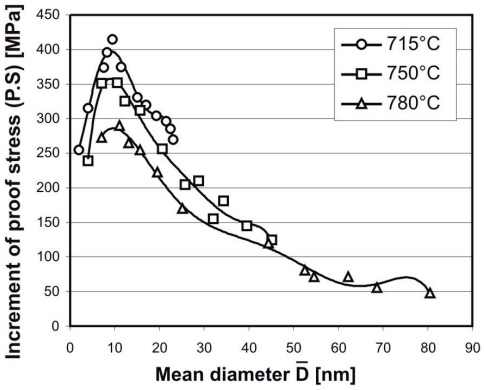

Fig. 12. Relations between increased proof stress and mean diameter of γ' precipitates

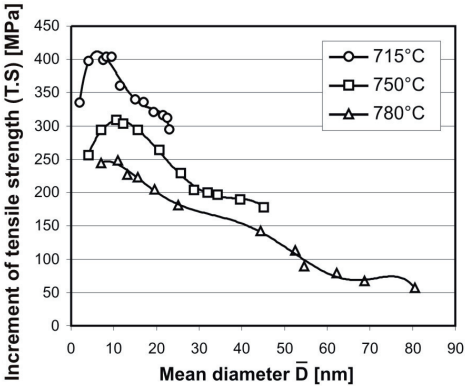

Fig. 13. Relations between increased tensile strength and mean diameter of γ' precipitates

$$\Delta\tau = \frac{\sigma_a}{M} \tag{6}$$

where: σ_a – increase in alloy yield point during ageing, M – Taylor's index (equals 3.06 for FCC structures).

The resultant values of the flow stress increase (Δτ) as a function of the mean diameter ($\overline{D}$) and square root ($\overline{D}$)$^{1/2}$ from the γ' phase precipitates that were presented in graphic form in Figs. 14 and 15. It is evident from these relationships that the highest increases in flow stress (Δτ = 129-136 MPa) were observed for the ageing temperature of 715°C and the heated equivalent diameter ($\overline{D}$) of the γ' phase particles of ca. 8-10 nm. Further increase in the particle diameters from 11 to 23 resulted in a rapid decrease in the strengthening level during ageing. For a higher ageing temperature (750°C), the greatest increases in flow stress (Δτ = 114-115 MPa) were obtained for the particle sizes of $\overline{D}$ = 7-11 nm. Further increase in the particle diameter was accompanied by a continuous decline of strength increase during ageing. For an ageing temperature of 780°C, the maximal increase of flow stress (Δτ = 89-95 MPa) occurred for the particle size of 7-11 nm. Further increase in the γ' precipitate sizes from 13 to 81 nm resulted in a lower rate of increase of flow stress of the tested alloy Fe–Ni.

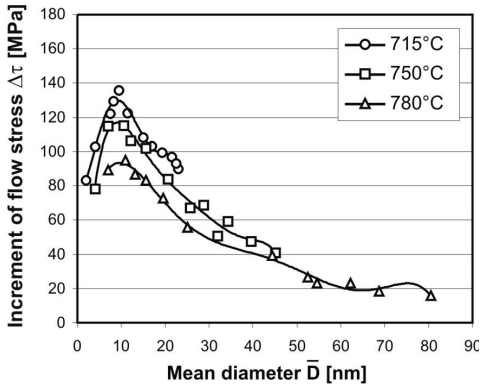

Fig. 14. Relations between increased flow stress and mean diameter of γ' precipitates

Similar relationships were observed for the increase of the flow stress as a function of the square root of the mean diameter $(\overline{D})^{1/2}$ of the γ' phase particles (Fig. 15).

Based on the results, it can be concluded that the greatest precipitation strengthening in the tested Fe–Ni alloy occurs at an ageing temperature of 715°C. A detailed graph of the alloy's flow stress increase (Δτ) as a function of the square root $(\overline{D})^{1/2}$ of the particle size was prepared for this temperature (Fig. 16).

It is evident from the figure that from short ageing times to the maximal strength of the alloy, the relationship between Δτ and the particle diameters $\overline{D}^{1/2}$ was linear. Such a relationship is typical for Fe–Ni alloys that have been precipitation strengthened [9]. The regression slope can be used in equation (5) to determine the APB energy. For the analyzed case, the APB energy in the tested Fe–Ni equalled ca. 210 mJ/m^2. This value is similar to the value of 225mJ/m^2, which was obtained by Thompson and Brooks [10] for a comparable Fe–Ni alloy of the A-286 type.

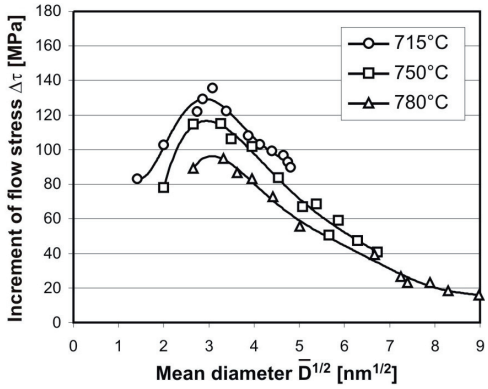

Fig. 15. Relations between increased flow stress and square root of mean diameter of γ' precipitates

4. Conclusions

Application of 1 × step ageing at 715, 750, and 780°C after heat solution treatment and holding times ranging from 0.5 to 500 h results in processes of precipitation of intermetallic phases of the γ'[$Ni_3(Al,Ti)$], η[Ni_3Ti], β[NiTi], G[$Ni_{16}Ti_6Si_7$], and σ[$Cr_{0,46}Mo_{0,40}Si_{0,14}$] types and of $M_{23}C_6$ carbide in the high-temperature Fe–Ni alloy of the A-286 type.

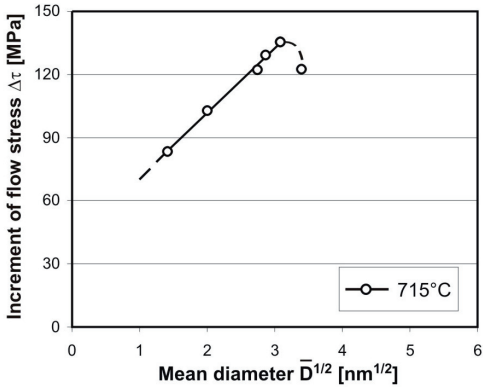

Fig. 16. Flow stress increment due to aging at 715°C as a function of square root of mean diameter of γ' precipitates

The intermetallic γ' phase was the primary phase precipitated during the ageing of the tested Fe–Ni alloy. Three characteristic stages can be distinguished in the process of γ' phase precipitation: coherent zones, coherent spheroidal particles($\overline{D}$ = 10 ÷ 35 nm) and coagulated spheroidal particles ($\overline{D}$ = 40 ÷ 80 nm). It was concluded that the mean diameter ($\overline{D}$) of the γ' phase precipitates increases as a function of the cube root of the ageing time ($t^{1/3}$), which is in conformity with predictions based on LSW theory for coagulation controlled by volume diffusion.

The processes of precipitation, growth, and coagulation of intermetallic phases and carbides occurring in the Fe–Ni alloy during aging had a significant impact on the alloy's mechanical properties. The greatest strengthening of the alloy was obtained at an aging temperature of 715°C. An increase in the aging temperature to 750 and 780°C was accompanied by clear effects of alloy overaging, which resulted in a decline in hardness and mechanical properties and a slight improvement of plastic properties.

It was observed that the level of strengthening obtained in the tested alloy significantly correlated with the γ' phase particle size and ageing temperature. The greatest strengthening of the alloy occurred in initial stages of aging for a mean diameter ($\overline{D}$) of the γ' phase particles ranging from 8 to 15 nm. A decrease in strengthening was observed for greater particle diameters, which is characteristic for the overageing process occurring in alloys that have been precipitation strengthened. Declining strengthening of the alloy with rising ageing temperature can be explained by lower density of the γ' phase precipitates caused by lower nucleation frequency and progress of the γ'→ η phase transition.

The analysis of flow stress increase (Δτ) as a function of the square root of the particle size $(\overline{D})^{1/2}$, which was carried out for the ageing temperature of 715, yielded a linear relationship to the peak of strength. The APB energy was determined by applying the conventional strengthening theory of Brown and Ham to the line regression slope; its value was estimated to be 210 mJ/m^2. This value is in agreement with values of APB obtained for similar Fe–Ni alloys.

Additional information

The presentation connected with the subject matter of the paper was presented by the authors during the 12th International Scientific Conference on Contemporary Achievements in Mechanics, Manufacturing and Materials Science CAM3S'2006 in Gliwice-Zakopane, Poland on 27th-30th November 2006.

References

[1] H.S. Jeong, J.R. Cho, H.C. Park, Microstructure prediction of Nimonic 80A for large exhaust valve during a hot closed dieforging, Journal of Materials Processing Technology 162 (2005) 504-511.

[2] S.A. Sajjadi, S.M. Zebarjad, Study of fracture mechanisms of a Ni-Base superalloy at different temperatures, Journal of Achievements in Materials and Manufacturing Engineering 18 (2006) 227-230.

[3] K.J. Ducki, Analysis of the structure and precipitation strengthening in a creep resisting Fe–Ni alloy, Journal of Achievements in Materials and Manufacturing Engineering 21 (2007) 25-28.

[4] I.M. Lifshitz, V.V. Slyozow, The kinetics of precipitation from supersaturated solid solution, Journal of Physics and Chemistry of Solids 19 (1961) 35-50.

[5] C. Wagner, Theory of transformation in sludge throw theresolution, Zeitschrift für Elektrochemie 65 (1961) 581-591 (in German).

[6] H. Gleiter, Fundamentals of Strengthening Mechanisms, Proceedings of the 6th International Conference on the Strength of Metals and Alloys, Melbourne, 3 (1982) 1009-1024.

[7] A.J. Ardell, Precipitation hardening, Metallurgical Transaction AIME, 16A (1985) 2131-2165.

[8] F.B. Pickering, Some aspects of the precipitation of nickel–aluminium–titanum intermetallic compounds in ferrous materials, Heat Treatment'73, The Metals Society, 1975, 391-401.

[9] L.M. Brown, R.K. Ham, Strengthening Methods in Crystals, Applied Science Publishers Ltd, London, 1971, 12-135.

[10] A.W. Thompson, J.A. Brooks, The mechanism of precipitation strengthening in an iron base superalloy, Acta Metallurgica 30 (1982) 2197-2203.

[11] A. Czyrska-Filemenowicz, B. Dubiel, K. Wiencek, Determination of the oxide particle density in ODS alloys means of transmission electron microscopy, Acta Stereologica 17/2 (1998) 225-236.

[12] A. Wasilkowska, M. Bartsch, U. Messerschmidt, R. Herzog, A. Czyrska-Filemenowicz, Creep mechanisms of ferritic strengthened alloys, Journal of Materials Processing Technology 133 (2003) 218-224.

[13] B. Dubiel, J. Wosik, H.J. Penkalla, A. Czyrska Filemonowicz, Quantitative TEM microstructural analysis of Ni-based superalloy Waspaloy, Proceedings of the Stereology and Image Analysis in Materials Science, Kraków, 2000, 135-140.

[14] J.H. Schröder, E. Arzt, Electron- microscopic investigation of dispersion-strengthened superalloys, Praktische Metallography 25 (1988) 264-273.

[15] K. Kusabiraki, Y. Takasawa and T. Ooka, Precipitation and Growth of γ' and η Phases in 53Fe–26Ni–15Cr Alloy, Iron and Steel Institute of Japan – ISIJ International 35 (1995) 542-547.

[16] K.J. Ducki, Precipitation and growth of intermetallic phase in a high-temperature Fe–Ni alloy, Journal of Achievements in Materials and Manufacturing Engineering 18 (2006) 87-90.